Anal Bioanal Chem
DOI 10.1007/s00216-009-3062-8

REVIEW

Fluorimetric characterization of single-walled carbon nanotubes

R. Bruce Weisman

Received: 6 July 2009 / Revised: 7 August 2009 / Accepted: 11 August 2009

Abstract Single-walled carbon nanotubes (SWCNTs) are a family of structurally related artificial nanomaterials with unusual properties and many potential applications. Most SWCNTs can emit spectrally narrow near-IR fluorescence at wavelengths that are characteristic of their precise diameter and chiral angle. Near-IR fluorimetry therefore offers a powerful approach for identifying the structural species present in SWCNT samples. Such characterization is increasingly important for nanotube production, study, separation, and applications. General-purpose and specialized instruments suitable for SWCNT fluorimetric analysis are described, and methods for interpreting fluorimetric data to deduce the presence and relative abundances of different SWCNT species are presented. Fluorescence methods are highly effective for detecting SWCNTs in challenging samples such as complex environmental or biological specimens because of the methods' high sensitivity and selectivity and the near absence of interfering background emission at near-IR wavelengths. Current limitations and future prospects for fluorimetric characterization of SWCNTs are discussed.

Keywords Single-walled carbon nanotube · Near-IR fluorescence · Fluorimetric analysis · Fluorimetry

Introduction

Single-walled carbon nanotubes (SWCNTs) are a class of artificial nanomaterials composed of carbon atoms that are covalently linked by sp^2 bonds and organized into extended tubular structures with long-range crystalline order. These nanotubes typically have diameters between 0.7 and 2 nm and lengths ranging from 100 nm to several micrometers (although they can also be grown to macroscopic lengths of many millimeters). SWCNTs are the subject of intense research interest because of their remarkable physical and chemical properties that suggest the potential for a wide variety of real-world applications, including several biomedical uses. Their networks of strong carbon-carbon bonds and tubular geometry lead to very high values of tensile strength and bending stiffness. SWCNTs offer maximal specific surface areas because all of the atoms are on the surface, as is also true for graphene. However, in contrast to graphene flakes, SWCNTs have no dangling bonds and are chemically stable without passivation.

SWCNT electronic and optical properties are perhaps the most unusual, as they vary strongly with the nanotube's physical construction [1]. Every possible SWCNT structure may be envisioned as a strip of planar graphene rolled up to form a seamless cylindrical tube with a particular diameter and chiral (or wrapping) angle. Each of these discrete structures can be labeled by a pair of integers, (n,m), that precisely define its diameter and chiral angle (Fig. 1). As a consequence of graphene's unusual π-electron band structure and the boundary condition imposed by the cylindrical nanotube geometry, structures for which the difference n-m is evenly divisible by 3 have metallic or semimetallic electronic characters, whereas the others are semiconducting. Statistically, two thirds of possible SWCNT structures are semiconducting, and among these the band gap is approximately inversely proportional to nanotube diameter. SWCNTs therefore form a class of all-carbon materials with electronic properties ranging from metallic through medium band-gap semiconducting. Nanotube optical properties

R. B. Weisman (✉)
Department of Chemistry and Richard E. Smalley Institute for Nanoscale Science and Technology, Rice University,
Houston, TX 77005, USA
e-mail: weisman@rice.edu

Published online: 08 September 2009

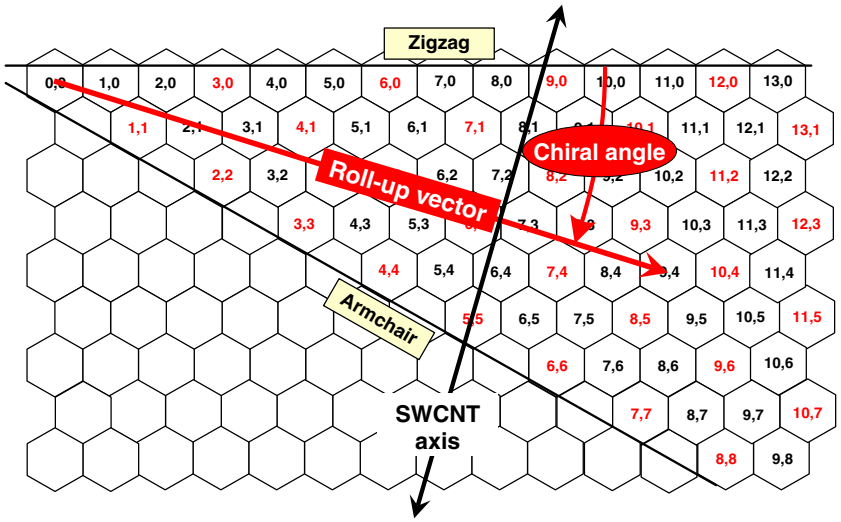

Fig. 1 The relation between single walled carbon nanotube (*SWCNT*) structure and graphene sheet roll-up. The roll-up vector connects position (0,0) to another labeled (*n*,*m*) position in the sheet [in this case (9,4)] and becomes the circumference of the resulting SWCNT. The nanotube diameter equals the length of its roll-up vector divided by π. Chiral angles are measured from the *line labeled zigzag* and range from 0° to 30°. Structures shown with *red labels* are metallic or semimetallic; those with *black labels* are semiconducting

naturally reflect the states available to the π electrons. The high aspect ratios of SWCNTs lead to quasi-one-dimensional electronic motion and pronounced peaks, resembling molecular orbitals, in the density of electronic states as a function of energy. Transitions between these van Hove singularities dominate the optical absorption and emission spectra.

A typical semiconducting SWCNT with diameter near 1 nm displays a series of well-defined optical absorption peaks, designated E_{11}, E_{22}, E_{33}, etc. that fall in the near-IR, visible, and near-UV regions, respectively. In a one-electron model of electronic structure, these absorptions correspond to optical excitations from a van Hove singularity in the valence band to the corresponding singularity in the conduction band. The precise spectral positions depend on both SWCNT diameter and chiral angle, with larger-diameter nanotubes generally absorbing at longer wavelengths. An important advance was reported in 2002, when it was found that SWCNTs also emit fluorescence, or photoluminescence, at their near-IR E_{11} transition wavelengths [2]. With the subsequent successful assignment of the E_{11} and E_{22} spectral transitions to specific (*n*,*m*) structures [3], optical spectroscopy has emerged as a promising approach for precise structural characterization of SWCNTs. Figure 2 shows a map of empirical E_{11} and E_{22} peak positions for a wide range of SWCNTs in aqueous suspension with sodium dodecyl sulfate or sodium dodecylbenzene sulfonate surfactant. The same data have also been used to construct an empirical "Kataura plot" of E_{11} and E_{22} optical transition energies vs nanotube diameter [4]. Because E_{33} and higher transitions are spectrally broader and not as thoroughly studied, they are less often used for (*n*,*m*) analysis.

Sample characterization is an essential task for basic and applied nanotube researchers. SWCNTs are grown by high-temperature decomposition of carbon-containing feedstocks catalyzed by metallic nanoparticles. Even with the best control of growth process conditions, nanotubes are formed as a variety of (*n*,*m*) structural species. The number of such species in a given SWCNT batch may range from a few to several dozen. Because many electronic, optical, chemical, and mechanical properties of SWCNTs depend on their structure, it is often important to know the identities and relative abundances of (*n*,*m*) species present in a sample. Several single-particle microscopic methods can be used to distinguish among (*n*,*m*) structures and determine their abundances. These include high-resolution scanning tunneling microscopy [5, 6] and electron nanodiffraction [7]. However, all of these techniques require expensive equipment, expert operators, and substantial measurement time. They are therefore impractical for the routine analysis of bulk samples. By contrast, fluorimetry offers a sensitive bulk method for assessing (*n*,*m*) contents. This paper will discuss the capabilities, limitations, and future prospects of fluorimetric analysis for detailed structural characterization of bulk SWCNT samples.

Instrumentation

The instrumentation appropriate for spectroscopic analysis of SWCNTs differs from standard absorption and emission spectrometers only because of the near-IR wavelengths needed to observe E_{11} transitions. The required near-IR spectral coverage varies with the source of SWCNTs to be analyzed. Two popular processes for chemical vapor deposition growth of SWCNTs are CoMoCAT, which uses CO feedstock with supported bimetallic Co-Mo catalyst particles [8], and HiPco, in which high-pressure CO is disproportionated on Fe nanoparticles formed in the gas phase from $Fe(CO)_5$ decomposition [9]. Both of these methods generate relatively small diameter nanotubes that

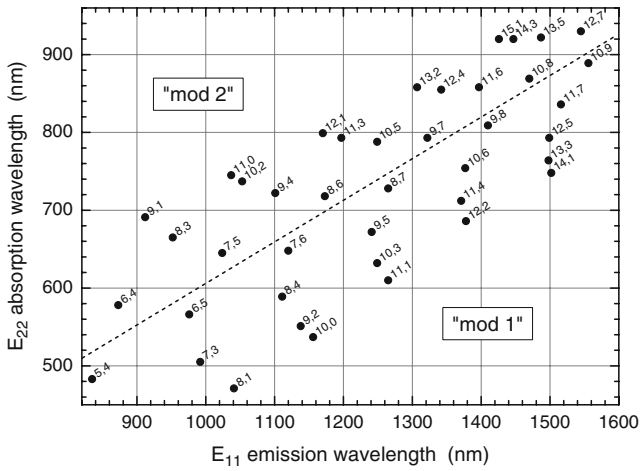

Fig. 2 Spectral map showing the peak E_{11} and E_{22} wavelengths for a range of SWCNT (*n*,*m*) species in aqueous sodium dodecyl sulfate or sodium dodecylbenzene sulfonate suspension. Peak positions are based on experimental data, not theoretical models. Species below the dashed line, labeled *mod 1*, give a remainder of 1 when the quantity *n*-*m* is divided by 3; those above the dashed line give a remainder of 2

have E_{11} transitions within the 850–1,600-nm range of standard InGaAs detectors [3, 10]. Nanotubes grown by the laser oven or arc discharge methods have larger average diameters and emit at wavelengths out to approximately 2,200 nm [11] , requiring the use of detectors such as extended-range InGaAs. The drawbacks of longer-wavelength detection include increased levels of noise, defective pixels, and response nonlinearities, plus the need for deeper cooling to suppress dark current.

Conventional general-purpose spectrofluorometers may be configured with cryogenic near-IR single-channel or multichannel detectors mounted on scanning monochromators or spectrographs to measure fluorescence from dispersed SWCNT samples. In such instruments, tunable excitation over the range of E_{22} transitions is typically provided by monochromatized visible-wavelength light from a high-pressure Xe arc lamp. By measuring emission spectra for a series of excitation wavelengths, one obtains a two-dimensional map in which each peak can be associated with a distinct (*n*,*m*) species of semiconducting SWCNT [3]. It is recommended that the near-IR emission data be supplemented by visible and near-IR absorption spectra to aid in sample analysis.

The sensitivity and data acquisition speed of general-purpose spectrofluorometers are limited by their low (often submilliwatt) excitation powers and inefficient optical geometries. These problems are overcome in a specialized instrument custom-designed for SWCNT fluorimetry (Fig. 3). Here fixed-wavelength diode lasers at selected wavelengths provide approximately 50 mW of excitation power that is tightly focused into a sample cell holding dispersed SWCNTs. Near-IR fluorescence is captured through a large solid angle centered at 180° to the excitation direction, and is then dispersed by a high-aperture transmissive spectrograph and detected by a thermoelectrically cooled multichannel InGaAs array to give 4-nm spectral resolution. The higher excitation power and efficient collection/detection optics provide a sensitivity enhancement of nearly 4 orders of magnitude compared with a general-purpose spectrofluorometer. Full-scale emission spectra (with signal-to-noise ratios approaching 10,000) can be acquired from well-dispersed SWCNT samples in as little as 25 ms. This high sensitivity allows near-IR fluorimetry to be used as a kinetic spectroscopy for studying structure-dependent chemical or physical transformations of SWCNTs. When a flowing sample cell is installed, the fast acquisition times also permit real-time monitoring of the composition of eluent streams (e.g., in chromatographs used for sample purification and sorting). Another benefit of a laser-based SWCNT fluorometer is the very small size of the focused excitation beam in the sample. This permits the use of minimal sample volumes of approximately 50 μL, or even less with specialized cells. Moreover, one can exploit the small beam size to measure spatially resolved fluorescence spectra of stratified layers inside undisturbed centrifuge tubes used to structurally sort SWCNTs by density-gradient ultracentrifugation. Finally, the optical design of the specialized SWCNT fluorometer also allows simple and near-simultaneous measurement of a sample's absorption spectrum. The combination of fluorescence and absorption data can be quite useful for studying SWCNT reactions and for incisive sample characterization (see below).

Methodology

Sample preparation is an important step in SWCNT fluorimetric analysis. Nanotubes have a strong tendency to aggregate into tight bundles bound by van der Waals forces. Electronic interactions within such bundles cause fluorescence quenching, so before fluorescence measurements are made it is necessary to disaggregate raw samples to obtain dispersions of individually suspended nanotubes, typically by ultrasonic agitation in aqueous surfactant solution [2]. In some surfactants, such as sodium dodecyl sulfate, it is also important to adjust the sample pH to an alkaline value to avoid acid quenching of SWCNT fluorescence [12, 13]. A convenient sample concentration is typically of order 1 mg of SWCNTs per liter or approximately 1 ppm by mass.

Once a properly dispersed sample has been prepared, its near-IR emission spectrum is measured as a function of excitation wavelength. When a general-purpose spec-

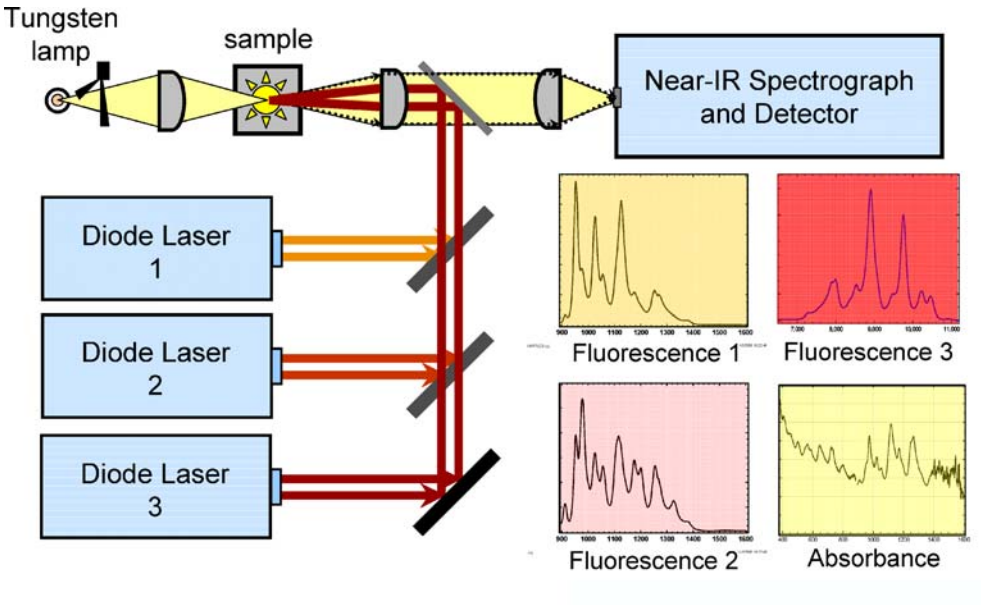

Fig. 3 Optical diagram of a specialized SWCNT fluorimeter. With the tungsten lamp blocked, the sample (in liquid dispersion) is excited sequentially by diode lasers at three different wavelengths, and the corresponding near-IR emission is collected at 180°, dispersed in a high-throughput spectrograph, and detected by a cooled InGaAs multichannel array. To measure the sample's absorption spectrum, the lasers are turned off, the tungsten lamp is unblocked, and the same detection system records the spectrum of near-IR light transmitted through the SWCNT sample. The result is compared with the transmission through a blank sample to obtain the absorption spectrum

trofluorometer is used, excitation should be scanned over a range wide enough to cover the E_{22} peaks of all SWCNT species present in the sample. Keeping in mind that the E_{11}/E_{22} wavelength ratios vary from approximately 1.3 to 2.1 [3], one can estimate this range from the sample's near-IR absorption spectrum and/or prior knowledge of its source and history. Each major peak in the resulting excitation-emission contour plot can be associated with a specific (*n*,*m*) species with the aid of tables of SWCNT spectral assignments [4]. Because peak positions shift slightly with changes in nanotube environment [14–16], it is advisable to use a standard surfactant for which tabulated precise spectral data are available. In addition to the primary peaks, which correspond to the tabulated spectral values, the contour plot will also show weaker peaks with the same emission wavelength but different excitation wavelengths. These are attributed to vibrational or excitonic sideband transitions of the (*n*,*m*) species that gives that primary peak [17–19]. By identifying all of the primary peaks in a sample's spectrum, one can straightforwardly compile a list of the semiconducting (*n*,*m*) species present in that sample.

Going beyond this qualitative analysis to find the quantitative distribution of (*n*,*m*) abundances is more involved. First, the raw emission intensities must be corrected for the instrument's wavelength-dependent excitation intensity and detection sensitivity. Then the results should be transformed from the wavelength units customarily used in data collection into optical frequency (cm^{-1}). Each primary (*n*,*m*) peak is spectrally integrated along the emission coordinate at its peak excitation value. This gives a set of relative fluorimetric signal strengths for the semiconducting (*n*,*m*) species. Converting these signal strengths into relative abundances requires some knowledge or assumptions about the (*n*,*m*) dependence of fluorimetric efficiencies (more technically, photoluminescence action cross sections). These photophysical parameters, which are the product of E_{22} peak absorption cross sections and fluorescence quantum yields, can vary systematically with SWCNT structure. Because there is little empirical knowledge of such efficiency variations, it has been customary to assume that they are equal, implying an (*n*,*m*) abundance distribution proportional to the fluorimetric signal strengths. Recently, however, values of photoluminescence action cross sections have been measured and reported for a significant number of (*n*,*m*) species, revealing variations exceeding a factor of 3 [20]. Ongoing research will provide a much larger set of these values in the near future. That result will finally allow relative abundances to be properly deduced from measured fluorimetric spectra, making SWCNT spectrofluorimetry the only bulk analysis method capable of measuring (*n*,*m*) distributions.

Although it might appear that the analysis described above requires the use of a general-purpose spectrofluorometer with continuously tunable excitation, equivalent information can also be obtained from specialized, laser-based SWCNT fluorometers. Such instruments generally excite the sample using three discrete excitation wavelengths. If the resonance windows for exciting specific (*n*,*m*) species were spectrally narrow, then this approach would fail to induce detectable fluorescence from most nanotubes in a typical sample. However, fluorescence from approximately 20 distinct (*n*,*m*) species can readily be detected using a single excitation wavelength (Fig. 4). This is true even for samples containing relatively small

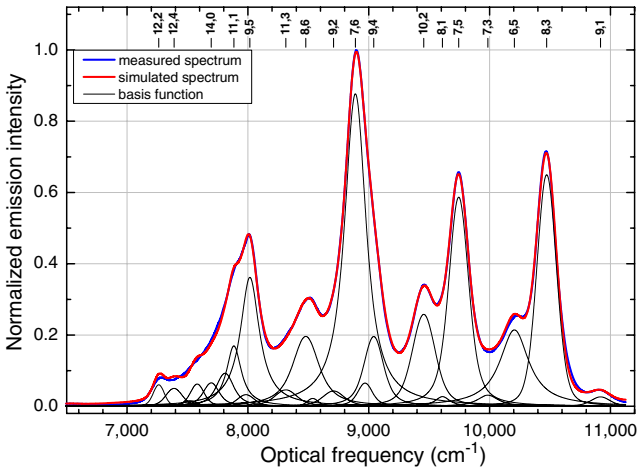

Fig. 4 Near-IR emission spectrum of a typical SWCNT sample as measured with a single excitation wavelength in approximately 50 ms using the instrument sketched in Fig. 3. The measured spectrum is simulated as a superposition of underlying fluorescence components from individual (*n*,*m*) species, which are shown as the *black curves*

diameter nanotubes with widely separated E_{22} peaks. The surprisingly large effective resonance widths in SWCNT fluorimetry arise from the long Lorentzian tails of the principal E_{22} peaks, plus many weaker spectral features from E_{22} vibronic sidebands, E_{11} vibronic sidebands, higher excitonic bands associated with E_{22}, and underlying continuum-like transitions. When emission is sensitively detected by a specialized SWCNT fluorometer, these relatively minor spectral absorptions lead to clear emission signatures of (*n*,*m*) species excited far from their principal E_{22} peaks. As a result, three properly chosen fixed excitation wavelengths have been found sufficient to allow detection of all semiconducting SWCNTs within a wide structural range.

Moreover, it is also possible to reconstruct the two-dimensional excitation-emission contour plot from the three emission spectra. This data analysis process requires prior knowledge of E_{11} and E_{22} spectral parameters for the set of semiconducting (*n*,*m*) species that may be present in the sample. Parameters include the positions, widths, and shapes of the principal E_{11} and E_{22} peaks; the positions and relative amplitudes of secondary spectral features; and the wavelengths and relative powers of the excitation lasers. Once these values have been determined or estimated, they are used to generate simulated near-IR emission spectra and the concentrations of all (*n*,*m*) species are treated as variable parameters and adjusted to simultaneously fit the three measured spectra. The high signal-to-noise ratio of the data exposes small deviations between experimental and simulated spectra during the fitting process, allowing sensitive optimization of some estimated spectral parameters in addition to the (*n*,*m*) concentrations. In this reconstruction of the two-dimensional contour plot from three one-dimensional slices, the relative optical excitation efficiency of an (*n*,*m*) species is computed from the spectral position of the excitation laser relative to the nanotube's E_{22} peak and its secondary absorption features. This procedure quantitatively accounts for the lower emission intensities from species that are excited off-resonance. With proper fitting, the set of (*n*,*m*) concentrations deduced using a small number of spectral slices (Fig. 5) agrees well with the results from a two-dimensional scan. The simple relation between SWCNT diameter and (*n*,*m*) indices, $d(\mathrm{nm}) = 0.0794\sqrt{n^2 + nm + m^2}$, makes it straightforward to construct a sample's diameter histogram once the relative (*n*,*m*) abundances are known (Fig. 6).

Comparison of fluorescence and absorption spectra provides another important method for characterizing SWCNT samples. Here the goal is not to deduce the (*n*,*m*) distribution, but instead to estimate the extent to which a sample contains individualized, pristine SWCNTs rather than aggregated, damaged, or multiwalled carbon nanotubes (MWCNTs), giant fullerenes, amorphous carbon, residual catalyst, or other impurities. The principle is that all of these undesired materials, as well as the "good" SWCNTs, absorb light, but only the individualized and undamaged SWCNTs emit near-IR fluorescence. The overall quantum yield of emission will therefore be greatest for the purest and best dispersed samples, and will be lowered by the presence of impurities or aggregates. To measure an "emissive index" value proportional to the quantum yield, one first spectrally integrates a sample's

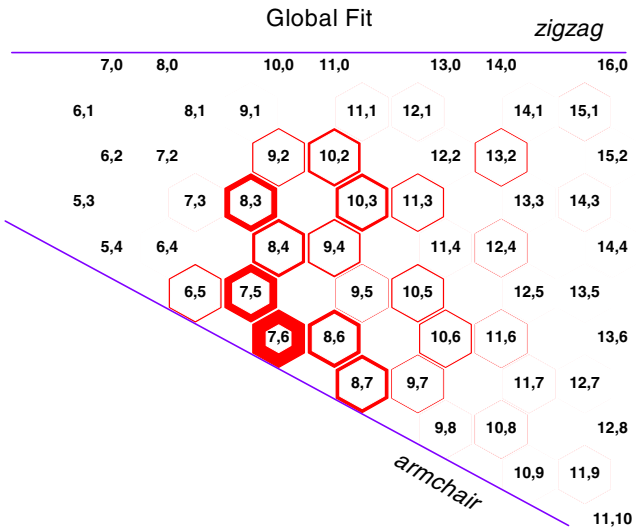

Fig. 5 Graphene sheet plot of the relative (*n*,*m*) abundances deduced by analysis of emission spectra measured using three discrete excitation wavelengths in the apparatus sketched in Fig. 3. The abundance of a given (*n*,*m*) species is proportional to the width of the colored hexagon surrounding its label

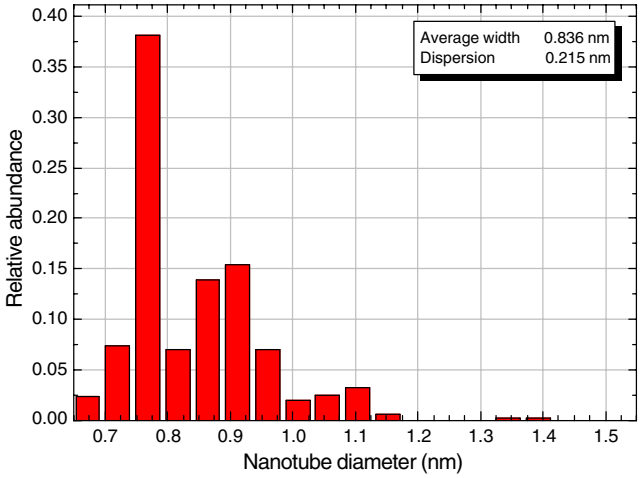

Fig. 6 Diameter histogram computed for a SWCNT sample, as based on (*n*,*m*) abundances deduced using the instrument sketched in Fig. 3

near-IR fluorescence spectrum. Then the integrated emission is divided by the sample's absorbance at the fluorescence excitation wavelength to obtain the sample's emissive index. If fluorescence is acquired using a general-purpose spectrofluorometer, a separate spectrophotometer will typically be needed to the measure sample's absorbance. However, the design of the specialized SWCNT fluorometer allows nearly concurrent measurement of both emission and absorption spectra in the same instrument, so a sample's emissive index can be determined and displayed within seconds under automatic software control. Note that emissive index values may vary from instrument to instrument because of differences in absolute fluorescence detection sensitivity, and they will also depend on the choice of excitation wavelength, surfactant, and general type of SWCNT sample that is being analyzed. The emissive index is therefore most useful within one laboratory for comparing samples of the same type that differ in preparation protocol or chemical processing. Because quenching of near-IR fluorescence is the earliest symptom of SWCNT bundling, one can sensitively detect even very minor aggregation in an unstable dispersion as an emissive index that declines steadily with time.

Near-IR fluorimetry provides the most effective approach for detecting nanotubes in complex environmental and biological specimens. Such specimens are often rich in carbon-containing compounds and biopolymers that can mask the presence of trace amounts of SWCNTs. Even expensive and labor-intensive microscopic methods such as high-resolution transmission electron microscopy can fail to distinguish nanotubes from nanoscale background objects. Among optical analysis methods, absorption spectroscopy has very low sensitivity and selectivity, but resonance Raman spectroscopy can successfully detect and image SWCNT accumulations in biological environments [21]. SWCNT fluorimetric detection offers several advantages over any other method. First, the emission is at near-IR wavelengths, for which both absorption and scattering by tissues are significantly lower than for visible light. Second, the E_{11} SWCNT emission can be efficiently induced by red light excitation of E_{22} transitions. The difference between excitation and emission wavelengths is therefore very large compared with the Stokes shifts of organic fluorophores, allowing convenient optical filtering and efficient detection. Third, SWCNTs display remarkably high photostability (resistance to bleaching and absence of blinking) under intense irradiation conditions [22, 23]. This property plus a short excited state lifetime allow a single illuminated SWCNT to undergo many rapid cycles of excitation and emission, giving a bright optical signal despite an emissive quantum yield no higher than a few percent. Finally and perhaps most importantly, the E_{11} emission range of approximately 850 to 1,600 nm is nearly free of autofluorescent background emission in most biological specimens. As a result of these factors, near-IR fluorescence is the most sensitive and selective method for microscopic or bulk detection of SWCNTs in complex environments [24, 25]. With use of a custom-built near-IR fluorescence microscope [20], it has been possible to detect, image, and structurally identify even individual SWCNTs in biological tissue specimens (Fig. 8) [26].

Capabilities and limitations

Full characterization of SWCNT samples is a complex, multifaceted task that requires a range of complementary measurements [27]. These might include thermogravimetric analysis for determination of catalyst and amorphous carbon content, high-resolution transmission electron microscopy imaging to check for non-SWCNT impurities, atomic force microscopy to assess length distributions, and Raman measurements of relative D and G band intensities to monitor covalent functionalization of nanotube sidewalls. Near-IR fluorimetry cannot replace these other characterization tools, but it does provide valuable additional information about the specific SWCNT diameters and chiral angles represented in the sample. Moreover, the measured fluorimetric signal strengths may also be converted into a quantitative (*n*,*m*) abundance distribution, now that structure-specific photoluminescence action cross sections are being measured and reported for use as calibration factors. This capability is unique to near-IR fluorimetry, as no other bulk analysis method can quantitatively deduce (*n*,*m*) abundances. For nearly a decade, Raman spectroscopy has been widely used to identify metallic and semiconducting SWCNT species from their diameter-dependent radial breathing mode frequencies [28].

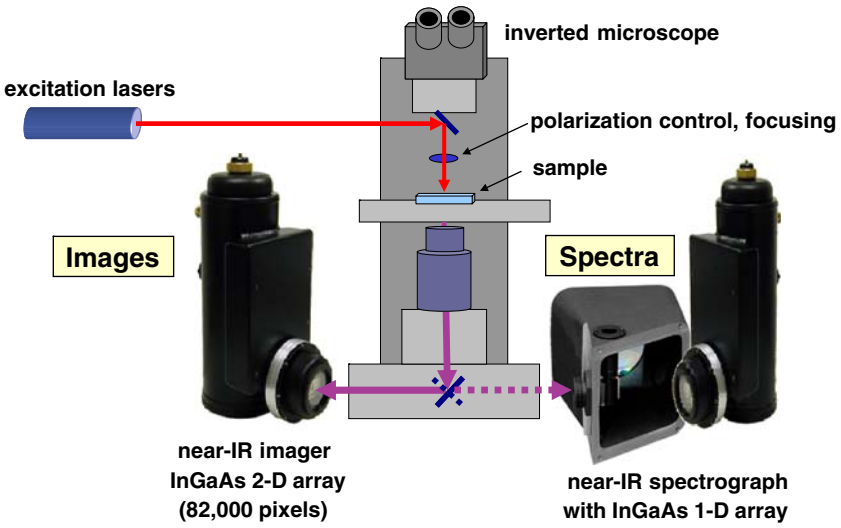

Fig. 7 Optical diagram of a near-IR fluorescence microscope designed for SWCNT studies. Samples are excited from above using fixed-wavelength diode lasers or a tunable dye laser. Emission is collected by the objective lens and imaged by a near-IR camera with a two-dimensional array of InGaAs pixels. Alternatively, emission light from a small region of the sample can be directed onto the slit of a near-IR spectrograph, where its spectrum is captured by a one-dimensional InGaAs array

However, these signals are observed only for nanotube species with electronic transitions falling within a rather narrow resonance window defined by the Raman excitation laser. A full qualitative analysis therefore requires so many Raman laser wavelengths as to be impractical for any normally equipped laboratory. It is even more challenging to deduce quantitative (*n*,*m*) abundance distributions from Raman data because structure-dependent scattering cross sections are not known.

The most obvious limitation of fluorimetric analysis is that it cannot detect metallic SWCNTs, which comprise roughly one third of the nanotubes in many samples. This prevents fluorimetric determination of the semiconducting-to-metallic ratio, an important property of interest for applications in electronics and conducting films. However, for the purpose of finding the distribution of physical structures in SWCNT samples, the invisibility of metallic species in fluorimetry may not be problematic. The reason is the likelihood that the same distributions of diameter and chiral angle describe both metallic and semiconducting SWCNTs from a single growth batch. Under this assumption, one can transfer the fluorimetrically determined structure distributions to deduce relative (*n*,*m*) abundances of metallic SWCNTs.

Another restriction involves the need for disaggregated and chemically pristine SWCNTs. Raw, as-produced nanotube samples do not show near-IR fluorescence because of bundling, and must be individualized by techniques such as ultrasonic agitation in surfactant solutions prior to fluorimetric analysis. Although this processing is not difficult, there is some possibility that the (*n*,*m*) distribution in the resulting suspension may not match the original sample distribution because of structure-dependent behaviors during processing. It will be necessary to explore this possibility by performing careful fluorimetric assays with a controlled range of processing protocols. Finally, there are several classes of carbon nanotubes that are unsuitable for fluorimetric analysis. SWCNTs that have undergone covalent sidewall functionalization will generally not show near-IR fluorescence because optically generated excitons are highly mobile and can be quenched

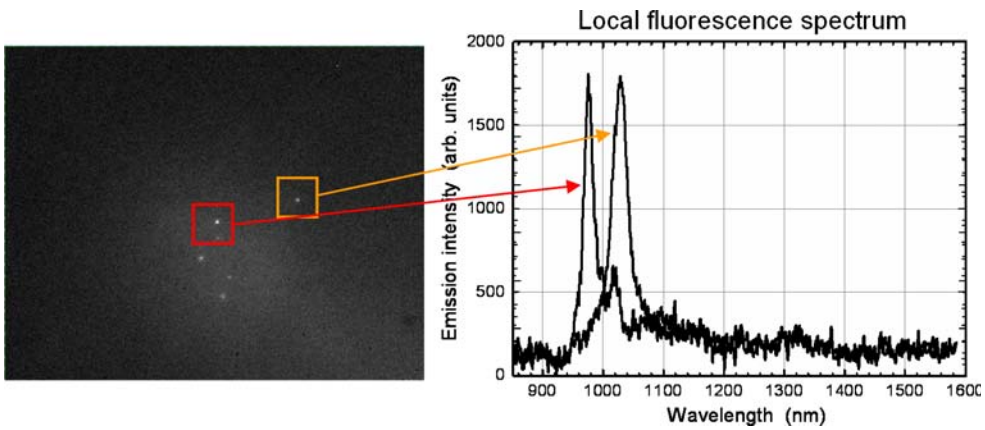

Fig. 8 Example of sensitive SWCNT detection in a biological sample. The *left frame* shows a nearh-IR emission image of dissected brain tissue from a *Drosophila* larva that had ingested SWCNTs in its food supply. Emission spectra of the two marked bright spots are displayed in the *right frame*. It is clear that each spot corresponds to an individual SWCNT [identified from spectra as (8,3) and (7,5) species] in the brain tissue. The data were acquired using the instrument sketched in Fig. 7

efficiently even by a low density of functionalized sites [29]. MWCNTs also show no detectable emission, presumably because of two factors: (1) their larger diameters shift the emission wavelengths deeper into the IR and reduce emissive quantum yields; and (2) nearly all MWCNTs contain at least one tube of metallic character that will accept energy and quench emission from other concentric shells in the MWCNT. Finally, there is currently no consensus as to whether the inner shells of double-walled carbon nanotubes emit near-IR fluorescence. A recent detailed study concludes that double-walled samples free of single-walled impurities show no such emission [30].

Future prospects

Fluorimetric analysis of SWCNTs should become more widely used and effective in the future because of several factors. First, steady advances in the controlled growth, purification, and structural sorting of SWCNTs demand improved characterization methods capable of (*n*,*m*)-level resolution. These are needed for tuning reactor conditions, checking product composition consistency, guiding the development of sorting techniques, and confirming the purity of sorted samples. Near-IR fluorimetric analysis is well suited to these tasks because it can be performed quickly by nonspecialists using modest instrumentation.

Enhanced effectiveness is expected in the future for the efficient laser-based SWCNT fluorometers that acquire a small number of emission spectra with fixed excitation wavelengths. Ongoing research studies are leading to improved understanding of nanotube spectroscopy that will enable refined modeling and fitting of emission spectra, allowing more accurate extraction of the individual (*n*,*m*) signal strengths. This process will also be improved by the identification and development of improved SWCNT surfactants that give sharper emission spectra and thereby reduce ambiguities from overlapping spectral features. Another boost to the value of fluorimetric analysis is the emerging knowledge of (*n*,*m*)-specific fluorimetric efficiency factors. These photophysical parameters allow the simple conversion of experimental fluorescence signal strengths into quantitative (*n*,*m*) abundance distributions. There is currently no other practical method for finding such abundance distributions.

Finally, near-IR fluorimetric methods should prove increasingly valuable in environmental and biomedical research studies involving carbon nanotubes. Trace amounts of SWCNTs in complex samples can be imaged in situ by near-IR fluorescence microscopy. Alternatively, they can be selectively detected and quantified by bulk near-IR fluorimetry of homogenized specimens or extracts prepared from them. As (*n*,*m*)-sorted SWCNT samples become increasingly available through techniques such as density-gradient ultracentrifugation [31], biomedical studies can be performed using nanotubes that are monodisperse in their optical properties. This will permit the use of very narrow spectral windows for excitation and emission, providing still higher levels of detection selectivity and sensitivity.

Acknowledgements The author is grateful to his current and former coworkers for their vital contributions to the research described in this paper. This work was supported by the National Science Foundation (grant CHE-0809020) and the Welch Foundation (grant C-0807).

References

1. Reich S, Janina J, Thomsen C (2004) Carbon nanotubes: basic concepts and physical properties. Wiley, New York
2. O'Connell MJ, Bachilo SM, Huffman CB, Moore V, Strano MS, Haroz E, Rialon K, Boul PJ, Noon WH, Kittrell C, Ma J, Hauge RH, Weisman RB, Smalley RE (2002) Science 297:593–596
3. Bachilo SM, Strano MS, Kittrell C, Hauge RH, Smalley RE, Weisman RB (2002) Science 298:2361–2366
4. Weisman RB, Bachilo SM (2003) Nano Lett 3:1235–1238
5. Odom TW, Huang JL, Kim P, Lieber CM (1998) Nature 391:62–64
6. Wildoer JWG, Venema LC, Rinzler AG, Smalley RE, Dekker C (1998) Nature 391:59–62
7. Qin L-C (2007) Phys Chem Chem Phys 9:31–48
8. Kitiyanan B, Alvarez WE, Harwell JH, Resasco DE (2000) Chem Phys Lett 317:497–503
9. Nikolaev P, Bronikowski MJ, Bradley RK, Rohmund F, Colbert DT, Smith KA, Smalley RE (1999) Chem Phys Lett 313:91–97
10. Bachilo SM, Balzano L, Herrera JE, Pompeo F, Resasco DE, Weisman RB (2003) J Am Chem Soc 125:11186–11187
11. Lebedkin S, Hennrich F, Skipa T, Kappes MM (2003) J Phys Chem B 107:1949–1956
12. Strano MS, Huffman CB, Moore VC, O'Connell MJ, Haroz EH, Hubbard J, Miller M, Rialon K, Kittrell C, Ramesh S, Hauge RH, Smalley RE (2003) J Phys Chem B 107:6979–6985
13. Weisman RB, Bachilo SM, Tsyboulski D (2004) Appl Phys A 78:1111–1116
14. Ohno Y, Iwasaki S, Murakami Y, Kishimoto S, Maruyama S, Mizutani T (2007) Phys Status Solidi B 244:4002–4005
15. Moore VC, Strano MS, Haroz EH, Hauge RH, Smalley RE (2003) Nano Lett 3:1379–1382
16. Choi JH, Strano MS (2007) Appl Phys Lett 90:223114-1–223114-3
17. Miyauchi Y, Oba M, Maruyama S (2006) Phys Rev B 74:205440–205440
18. Lefebvre J, Finnie P (2007) Phys Rev Lett 98:167406-1–167406-4
19. Murakami Y, Lu B, Kazaoui S, Minami N, Okubo T, Maruyama S (2009) Phys Rev B Condens Matter Mater Phys 79:195407-1–195407-5
20. Tsyboulski DA, Bachilo SM, Weisman RB (2005) Nano Lett 5:975–979
21. Zavaleta C, De La Zerda A, Liu Z, Keren S, Cheng Z, Schipper M, Chen X, Dai H, Gambhir SS (2008) Nano Lett 8:2800–2805

22. Tsyboulski DA, Bachilo SM, Kolomeisky AB, Weisman RB (2008) ACS Nano 2:1770–1776
23. Heller DA, Baik S, Eurell TE, Strano MS (2005) Adv Mater 17:2793–2799
24. Cherukuri P, Bachilo SM, Litovsky SH, Weisman RB (2004) J Am Chem Soc 126:15638–15639
25. Cherukuri P, Gannon CJ, Leeuw TK, Schmidt HK, Smalley RE, Curley SA, Weisman RB (2006) Proc Natl Acad Sci USA 103:18882–18886
26. Leeuw TK, Reith RM, Simonette RA, Harden M, Cherukuri P, Tsyboulski DA, Beckingham KM, Weisman RB (2007) Nano Lett 7:2650–2654
27. Freiman S, Hooker S, Migler K, Arepalli S (2008) Measurement issues in single wall carbon nanotubes. NIST special publication 960-19. US Government Printing Office, Washington
28. Dresselhaus MS, Dresselhaus G, Saito R, Jorio A (2005) Phys Rep 409:47–99
29. Cognet L, Tsyboulski D, Rocha J-DR, Doyle CD, Tour JM, Weisman RB (2007) Science 316:1465–1468
30. Tsyboulski D, Hou Y, Fakhri N, Ghosh S, Zhang R, Bachilo SM, Pasquali M, Chen L, Liu J, Weisman RB (2009) Nano Lett doi:10.1021/nl901550r
31. Arnold MS, Green AA, Hulvat JF, Stupp SI, Hersam MC (2006) Nature Nanotech 1:60–65